PCCP

Supramolecular aggregates formed by L-glutamic acid-oligomers: SANS and SAXS studies of the hydrogen bonded self-assembly

M. Ishida,[a] M. Takai,[a] H. Okabayashi,*[a] H. Masuda,[a] M. Furusaka[b] and C. J. O'Connor[c]

[a] *Department of Applied Chemistry, Nagoya Institute of Technology, Gokiso-cho, Showa-ku, Nagoya, 466-8555 Japan*
[b] *Neutron Science Laboratory, Institute for Materials Structure Science, High Energy Accelerator Research Organization, Oh-ho 1-1, Tsukuba, 305-0801 Japan*
[c] *Department of Chemistry, The University of Auckland, Private Bag 92019, Auckland 1, New Zealand*

Received 19th January 2001, Accepted 1st June 2001
First published as an Advance Article on the web 12th July 2001

N-Acetyl-L-glutamic acid oligomeric benzyl esters with various residue numbers (N_p = 4, 5, 6, 8, 10, 12 and 14) have been synthesized by a stepwise procedure. The microstructures of these oligopeptide aggregates in dioxane or benzene have been investigated by IR, small angle neutron scattering (SANS), and small angle X-ray scattering (SAXS) spectra. It has been confirmed from the IR spectral data that preferential stabilization of antiparallel-type β-sheet structures occurs above the critical aggregation concentration and that the population of this antiparallel β-sheet increases with an increase in concentration. On the basis of these IR results, the model of the rod-like aggregate, in which the disk-like β-sheet monomers are one-dimensionally stacked antiparallel to each other, has been presented for analysis of the observed SANS and SAXS intensity profiles. The best fit intensity profiles, calculated with variation only of the aggregation number and with fixed molecular parameters based on the assumption of polydispersity, have furnished the monomer–monomer bond energies ($\alpha\kappa T$), corresponding to the hydrogen bonding energies, the number-average aggregation numbers, and the number-average molecular weights for these oligopeptide aggregates. Thus, the rod-like aggregates, formed by these oligopeptides in dioxane or benzene, can be regarded as supramolecular aggregates.

Introduction

It should be emphasized that the conformational change of molecules upon aggregation or dissociation has a fundamental significance, since it provides an important model for the relationship between the functional appearance and the conformational change of biological molecules. In particular, conformational studies of surfactant molecules in the aggregated state assist in our understanding of the physicochemical properties of biological systems with respect to their relationship to an aggregated structure.

Okabayashi *et al.*[1–5] have demonstrated that one specific isomer, of all the possible rotational isomers about the CH_2–CH_2 single bond or the CH_2–CH single bond adjacent to the C=C double bond of simple saturated or unsaturated surfactant molecules, is preferentially stabilized upon micellization. Such a conformational change, due to the formation of micelles, has been found for the peptide bond (C⁻⁻N) of an amino acid surfactant, sodium *N*-acylsarcosinate, which exists in both the *cis* (**I**) and *trans* (**II**) conformations about the C⁻⁻N bond in aqueous solution:

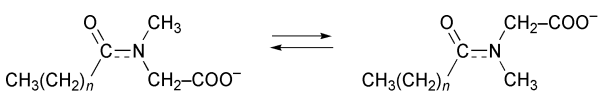

I **II**

We have found that micellization induces preferential stabilization of the *trans* form,[6,7] indicating that the hydrophobic interaction is the only driving force for the conformational change about the peptide group. Furthermore, we have confirmed that aggregation of *N*-acylglycine oligopeptides in water also brings about preferential stabilization of a specific conformer about the peptide C⁻⁻N bond, in which hydrogen bonding, in addition to the hydrophobic interaction, plays a critical role in its stabilization.

Becker *et al.*[8] and James *et al.*[9] showed that the stereochemistry and the self-association of *N*-urethanyl amino acids may be significant in enzymatic and synthetic reactions.

Proteins, which may be regarded as one class of very complex amphiphilic molecules, are compacted into giant self-organized systems. Beaudette *et al.*[10,11] have found that a conformational change upon formation of a giant aggregate occurs in complexes of histone proteins.

Doty *et al.*[12] presented high molecular weight poly-γ-benzyl-L-glutamate (PBLG) as a model molecule for proteins which take up an α-helical conformation, even in some organic solvents, as well as in the solid state. Wada[13] suggested a model for an α-helical PBLG aggregate, in which side-by-side random orientation and head-to-tail types are superimposed, as the most possible association of the PBLG α-helix in the dioxane–dimethylformamide mixed solvent. Tadmor *et al.*[14] studied the state of aggregation of helical PBLG in concentrated solutions and gels by SANS and SAXS methods, showing that, for the mechanism of gelation in the α-helical PBLG–benzyl alcohol system, the solvent plays a critical role.

Doty *et al.*[12] suggested, as early as 1956, that very low molecular weight PBLG takes up the intermolecular hydrogen bonded β-form in the aggregated state in weakly interacting solvents.

High molecular weight PBLG has its intramolecular hydrogen bonds in a rigid α-helical structure, while low molecular

 DOI: 10.1039/b100717n

weight PBLG has an intermolecular hydrogen bonding network in a β-sheet structure. This marked difference in the manner of hydrogen bonding seems to provide the difference in their aggregated structures.

Although exhaustive research on high molecular weight PBLG solutions has been carried out for more than forty years by various methods, the converse is true with respect to physicochemical studies of low molecular weight PBLG solutions. In particular, studies on the oligopeptides are relatively few compared with those for high molecular weight PBLGs.

A number of studies have been reported on the association of cyclic peptides made up of alternating D- and L-amino acids. These show that rings of cyclic peptides can be self-assembled to tubular structures,[15] dimers,[16] or ion channels.[17]

The microstructure of such oligopeptide aggregates and the mechanism of the aggregation process still remain unresolved and further investigation of them is highly desirable if we are to elucidate the various significant problems remaining unresolved in proteins.

In this present study, a series of *N*-acetyl-L-glutamic acid oligomeric benzyl esters [residue number (N_p) = 4, 5, 6, 8, 10, 12 and 14] and of *N*-octanoyl-L-glutamic acid oligomer benzyl esters (N_p = 6, 8 and 12) with exact residue numbers (not averaged over the degree of polymerization) have been synthesized by a stepwise procedure, and the microstructures of the aggregates formed by these oligomers in dioxane and benzene have been studied by use of IR, SANS and SAXS spectra.

Experimental

Materials

N-Acetyl- and *N*-octanoyl-L-glutamic acid benzyl ester oligopeptides were prepared by a stepwise procedure as follows. *N*-*tert*-butoxycarbonyl-L-glutamic acid α,γ-dibenzyl ester oligomers (BOC–Glu oligomer dibenzyl esters) were prepared from *N*-*tert*-butoxycarbonyl-L-glutamic acid γ-dibenzyl ester and L-glutamic acid α,γ-dibenzyl ester toluene *p*-sulfonate in dichloromethane in the presence of triethylamine. The usual *N*,*N*′-dicyclohexylcarbodiimide (DCCD) method[18] was used for the condensation reaction. For the BOC–Glu oligomeric benzyl esters thus obtained, confirmation of the residue number (N_p) was made by proton NMR: the value of N_p was obtained from the relative peak areas of the BOC CH_3 ^{1}H NMR signal and those of the benzyl protons. The BOC groups of these oligomers were removed by the action of hydrogen chloride in ethyl acetate. The BOC-free oligomeric benzyl esters were coupled with acetic acid and octanoic acid, respectively, by the DCCD method in dichloromethane.

The samples thus prepared were recrystallized in dichloromethane–petroleum ether. The residue numbers (N_p) of the *N*-acetyl-L-glutamic acid oligomer benzyl esters (AN_pZ), $CH_3CO[NHCH(CH_2CH_2CO_2\text{-benzyl})CO]_{N_p}O$-benzyl, synthesized for the present study, were 4, 5, 6, 8, 10, 12 and 14 (abbreviations: A4Z, A5Z, A6Z, A8Z, A10Z, A12Z and A14Z, respectively), and those of the *N*-octanoyl-L-glutamic acid oligomer benzyl esters (ON_pZ), $CH_3(CH_2)_6CO$-$[NHCH(CH_2CH_2CO_2\text{-benzyl})CO]_{N_p}O$-benzyl, were 6, 8 and 12 (abbreviations: O6Z, O8Z and O12Z, respectively).

The critical aggregation concentrations (c.a.c.) of the AN_pZ solutes in 1,4-dioxane [abbreviation: dioxane], which were obtained from the light-scattering data for A4Z, A6Z, A8Z and A12Z, are c.a.c. > 0.05 g ml^{-1} for A4Z, 0.01 g ml^{-1} for A5Z, 0.005 g ml^{-1} for A6Z, and c.a.c. < 0.001 g ml^{-1} for A8Z and A12Z. *N*-*tert*-Butoxycarbonyl-L-glutamic acid γ-benzyl ester and L-glutamic acid α,γ-dibenzyl ester toluene *p*-sulfonate were purchased from the Peptide Institute Inc. (Osaka, Japan). Deuteriated 1,4-dioxane [abbreviation: dioxane(d8)] and benzene, purchased from Aldrich Chemical Company, were distilled in the presence of CaH_2 and were used for preparation of the sample solutions after confirming the absence of H_2O from the absence of an IR band at 3500 cm^{-1}.

X-ray powder diffraction pattern and IR spectral measurements

X-ray powder diffraction patterns were obtained by the use of an RAD-RC diffractometer with counter-monochromator (CuKα, 50 kV, 110 mA). IR spectra were recorded on a Perkin-Elmer 1600 FTIR spectrometer (4000–400 cm^{-1}) with the sample dispersed in KBr disks for the solid states and with the sample–dioxane (or benzene) solutions sandwiched between two CaF_2-plate windows (spacer 0.015–0.5 mm).

^{1}H NMR measurements

^{1}H NMR spectra were recorded on a Varian XL-300 spectrometer operating at 300.112 MHz for protons (spectra) width of 4500.5 Hz, 32 768 points in the time domain, acquisition time of 3.641 s and delay of 8.359 s at 25.0 °C. NMR sample tubes (5 mm) were used for these measurements.

Molal volume determination

The apparent molal volumes (Φ_{app}) of these oligomers were calculated from the densities of the sample–dioxane solutions by using eqn. (1a)

$$\Phi_{app} = (1/m)[(1000 + mM)/\rho - 1000/\rho_s] \quad (1a)$$

$$\Phi_{app} = \Phi^0 + A_v m \quad (1b)$$

where m is the molality of the solution in units of mol kg^{-1}, M is the molecular weight of the solute, and ρ and ρ_s are the densities of the solution and of the solvent in units of g cm^{-3}, respectively. A_v is the experimental slope and Φ^0 is the infinite dilution molal volumes of the solutes. The Φ^0 values were obtained by least-squares fitting of the Φ_{app} values to eqn. (1b). The densities of the sample solutions were measured with a Lipkin-Davison type pycnometer calibrated with the known density of water at 298.15 ± 0.02 K. The Φ^0 values thus obtained are 821.3 cm^3 mol^{-1} for A4Z, 993.7 cm^3 mol^{-1} for A5Z and 1161.2 cm^3 mol^{-1} for A6Z, providing a linear relationship (Φ^0 = 142.2 + 170.0 N_p) between Φ^0 and N_p. The Φ^0 values of 260.9 cm^3 mol^{-1} (ref. 19) for the octyl and *O*-benzyl (OBz) moieties and of 170.0 cm^3 mol^{-1} for the –Glu(OBz)– moiety were evaluated.

Small angle neutron and X-ray scattering measurements

The small angle neutron scattering (SANS) measurements were carried out using the SAN instrument (with quartz cell of 1 mm path length and with a sample-to-detector distance of 3 m) and the medium angle neutron scattering instrument (WINK) (with quartz cell of 2 mm path length) installed at the pulsed neutron source KENS at the High Energy Accelerator Research Organization, Tsukuba, Japan. The SANS instrument (SANS-U) installed at the JRR-3M reactor at the neutron scattering laboratory in the Institute for Solid State Physics of the University of Tokyo, Tokai, Japan, was also used for SANS measurements with a quartz cell of 4 mm path length and camera length of 1 m and 4 m. The intensity of the scattered neutrons was recorded on a position-sensitive 2D detector.

The scattering length density (ρ) of each component was calculated using the equation

$$\rho = \sum_i b_i/V \quad (2)$$

where b_i is the scattering length of atom i and V is the molecular volume. The V values, calculated from partial molar

volume data measured in this present study, and the $\sum b_i/V$ values quoted from ref. 20, were used. The V values of A6Z, as a representative of AN_pZ and ON_pZ, dioxane and dioxane(d8) are 1161.2, 141.5 and 141.3 Å^3, respectively, and neutron scattering length densities of A6Z, dioxane and dioxane(d8) are 1.98, 0.59 and 6.49 × 10^{-6} Å^{-2}, respectively. The magnitude of the momentum transfer (Q) is given by

$$Q = \frac{4\pi}{\lambda}\sin\left(\frac{\Theta}{2}\right) \tag{3}$$

where Θ is the scattering angle and λ is the incident wavelength (3–11 Å for SAN, 1–16 Å for WINK, and 5 Å for SANS-U).

The scattering intensity from the sample solutions was corrected for detector background and sensitivity, empty cell scattering, incoherent scattering, and sample transmission. Solvent intensities were subtracted from those of the samples. The resulting corrected intensities were then radially averaged to give values of the relative scattering intensity *vs.* Q. Normalization of the data was made by using the scattering spectrum and transmission of a 1 mm water sample for SAN and WINK, and by using those of luporene for SANS-U.

The small angle X-ray scattering (SAXS) measurements were carried out with a quartz cell of 1 mm path length and incident X-ray wavelength of 1.49 Å using the small angle X-ray scattering spectrometer for enzymes, installed at the BL10C (or BL15A) line of the 2.5 GeV storage ring in the Photon Factory at the High Energy Accelerator Research Organization, Tsukuba, Japan.

Theoretical background for SANS and SAXS analyses

In the one-dimensional rod-like aggregation model,[21] in which identical disk-like molecules are stacked and make up a linear chain, we may define the bond energy (in this present study, hydrogen bonding energy) between the monomer and the monomer in the aggregate, relative to isolated monomers in solution, as equal to $\alpha\kappa T$ (κ is the Boltzmann constant and T is absolute temperature).

The density distribution function (D) of molecules in aggregates consisting of i molecules is given by

$$D_i = i[1 - (1/\sqrt{fe^a})]^i e^{-a}/f \tag{4}$$

where f is the molal fraction of the solute. This equation is restricted to dilute systems in which the inter-aggregate interactions can be ignored.

Since this density function (D_i) takes the maximum i value (i_{max}) at $\partial D_i/\partial i = 0$, i_{max} is expressed as:

$$i_{max} = \sqrt{fe^a} = N_n \tag{5}$$

i_{max} is equal to the number-average aggregation number (N_n). Thus, the monomer–monomer bond energy $\alpha\kappa T$ in the one-dimensional aggregation model can be calculated from

$$\alpha\kappa T = [\ln(N_n^2/f)]\kappa T \tag{6}$$

The dependence of the neutron or X-ray scattering intensity $d\Sigma(Q)/d\Omega$ on the magnitude of the scattering vector (Q) can be expressed as a function of both the particle structure factor $P(Q)$ and size- and orientation-weighted interparticle structure factor $S'(Q)$, as follows:

$$d\Sigma(Q)/dQ = I_0\,P(Q)S'(Q) \tag{7}$$

where I_0 is the extrapolated zero-angle scattering intensity, which is independent of the Q value. I_0 is a function of the number-average aggregation number N_n and is expressed by eqn. (8) in terms of the volumes of the aggregate (V_m, in Å^3) and the average neutron or electron scattering length densities of the aggregate and the solvent (ρ_m and σ_s, in Å^{-2}, respectively):

$$I_0 = \frac{CN_AV_m^2(\rho_s - \rho_m)^2 \times 10^{-16}}{1000n} \tag{8}$$

where n and C are the aggregation number and the concentration (mol l^{-1}), respectively, and N_A is Avogadro's number.

When interactions between aggregates are neglected, as in the case with dilute non-ionic aggregate systems in organic solvents, the interparticle structure factor is reduced to unity [$S'(Q) = 1$]. Therefore, eqn. (7) is given by

$$d\Sigma(Q)/d\Omega = I_0\,P(Q) \tag{9}$$

When the cross-section of a rod-like aggregate is circular, the particle structure factor, $P_i(Q)$, of an aggregate with aggregation number i can be calculated by

$$P_i(Q) = \int_0^{\pi/2} \frac{\sin^2[Q(Hi/2)\cos\beta]}{Q^2(Hi/2)^2\cos^2\beta}\,\frac{4J_1^2(Qr\sin\beta)}{Q^2r^2\sin^2\beta}\sin\beta\,d\beta \tag{10}$$

where i is the number of stacked circular disks (that is, the aggregation number), H is the thickness (Å) of a circular disk, r is the radius of the circular disk and J_1 is the first-order Bessel function.

When a rod-like aggregate has an elliptical cross-section, $P_i(Q)$ can be calculated by

$$P_i(Q) = \int_0^{\pi/2} d\beta \int_0^1 \frac{\sin^2[Q(Hi/2)\cos\beta]}{Q^2(Hi/2)^2\cos^2\beta}\,\frac{4J_1^2(Qr_e\sin\beta)}{Q^2r_e^2\sin^2\beta}\sin\beta\,d\mu \tag{11}$$

where $r_e = r\sqrt{\xi^2\mu^2 + (1-\mu)^2}$, i is the number of stacked elliptical disks, H is the thickness (Å) of an elliptical disk, r is the minor axis of an ellipsoid, ξ is the axis ratio and J_1 is the first-order Bessel function.

When we assume that the aggregates of AN_pZ and ON_pZ are in a polydispersed state, the neutron (or X-ray) scattering intensity can be expressed as:

$$\frac{d\Sigma(Q)}{d\Omega} = \frac{N_A(\rho_s - \rho_m)^2 \times 10^{-16}}{1000}\sum_i^\infty \frac{C_iV_i^2}{i}P_i(Q) \tag{12}$$

where $C_i(=CD_i)$ is the concentration (mol l^{-1}) of an aggregate with aggregation number i. Furthermore, since $V_i = iV_{mo}$ [V_{mo} is the volume (Å^3) of the monomer],

$$\frac{d\Sigma(Q)}{d\Omega} = \frac{N_AV_{mo}^2(\rho_s - \rho_m)^2 \times 10^{-16}}{1000}\sum_i^\infty C_iiP_i(Q) \tag{13}$$

when we define the dimensionless function $P(Q)$ as

$$P(Q) = \frac{\sum_{i=1}^\infty C_iiP_i(Q)}{\sum_{i=1}^\infty C_ii} \tag{14}$$

Thus, the scattering intensity $d\Sigma(Q)/d\Omega$ [or $I(Q)$] can be expressed as

$$\frac{d\Sigma(Q)}{d\Omega} = \left[\frac{N_AV_{mo}^2(\rho_s - \rho_m)^2 \times 10^{-16}}{1000}\sum_i^\infty C_ii\right]P(Q) \tag{15a}$$

$$I(Q) = AP(Q) \tag{15b}$$

where $A \equiv$ scaling factor [averaged values of (observed scattering intensity)/$P(Q)$].

In the present analyses, for the oligomers with N_p = 4–8 a circular disk was assumed and for those with N_p = 10–14 an elliptical disk was assumed. It was assumed that the thickness, H, of a circular (or elliptical) disk corresponds to the distance between the β-sheet type peptide chains, which are commonly observed in the X-ray powder diffraction patterns of these

solid oligomers. The radius (r) of a circular disk was calculated from the equation $r = \sqrt{V/(H\pi)}$ (H is the thickness of a circular disk and V is the molecular volume obtained from the partial molal volume measurements). The axis ratios (ξ) for an elliptical disk were calculated from the molecular model. Molecular parameters used for calculations of the intensity profiles are listed in Tables 1 and 2.

The present analysis has been carried out by use of eqn. (15b) as follows. In the calculation of $P(Q)$, the values of H and r, listed in Tables 1 and 2, were fixed and the number-average aggregation number (N_n) was varied as a fitting parameter. The scaling factor A, which can be calculated from the observed scattering data at all Q, was not used as an adjustable parameter in fitting the scattering intensity data. Thus, the $I(Q)$ value has been determined from the A value and the $P(Q)$ as a function of N_n, implying that $I(Q)$ can be calculated as a function of the aggregation number N_n. Finally, the value of N_n that minimizes the error calculated from $I(Q)$ and the observed scattering intensity was obtained.

Results

We have reported phase diagrams and phase structures for the *N*-octanoyl-L-glutamic acid oligomer benzyl esters–$CHCl_3$ systems and IR evidence for the conformational change of the oligomer molecules upon aggregation in chloroform.[22] Results of special relevance to this present study may be summarized as follows.

N-Octanoyl-L-glutamic acid oligomeric benzyl esters (residue number $N_p = 3$, 4, 6, 8 and 12) have been synthesized by a stepwise procedure. For all the solid samples, X-ray powder diffraction patterns and vibrational spectroscopic measurements have led to the assumption of an antiparallel-chain pleated β-sheet structure. For the chloroform solutions of the tetramers, hexamers and octamers, the phase diagram consists of three regions (I, II and III). Region I is an anisotropic phase, in which the aggregate structure strongly depends upon concentration, and Region II is a lyotropic liquid crystal area. Region III is a two-phase area in which Regions I and II coexist. For the oligomers with $N_p = 3$–12 in Region I, aggregation induces preferential stabilization of the β-sheet structure, depending upon the concentration. Further stabilization of the β-sheet structure and its growth occur in Region II.

The X-ray powder diffraction patterns were measured for the solid AN_pZ samples, used in this present study. Lattice spacings were observed in common at 4.71–4.74 Å and 15.53 Å, which can be assigned to the distance between β-sheet-type peptide chains and the side-chain spacing, respectively.[23] Thus, X-ray powder diffraction patterns provided ample evidence that the series of AN_pZ oligomers takes up a β-sheet structure in the solid state.

For the antiparallel β-sheet structure of synthetic polypeptides in the solid state, the band frequencies observed for amide I components are reflected essentially by the properties of the backbone structure of polypeptide.[24,25] For the IR spectra of the solid β-sheet polypeptides, the $\nu(0, \pi)$ and $\nu(\pi, 0)$ modes for the amide I frequencies are usually observed at 1685–1705 and 1615–1637 cm^{-1}, respectively, and the mean value of the split separation is 67 cm^{-1} (ref. 25). The amide I modes characteristic of the β-sheet are useful for study of the conformation of AN_pZ in dioxane or benzene.

We have investigated phase behaviors and molecular conformations of *N*-acetyl-L-glutamic acid oligomeric benzyl esters ($N_p = 4$, 5, 6, 8, 10, 12 and 14) in dioxane and benzene, by the use of near-IR and IR spectra (to be reported separately). Fig. 1 shows the IR spectra of the A10Z dioxane solutions as a representative of the AN_pZ series in the 1500–1800 cm^{-1} region. The IR bands at 1624 and 1692 cm^{-1} are assigned to the $\nu(0, \pi)$ and $\nu(\pi, 0)$ modes of amide I vibration for the antiparallel-type β-sheet structure. The amide I split separation ($\Delta\nu$) is $\Delta\nu = 68$ cm^{-1} and completely coincides with that (67 cm^{-1}) of the polypeptides.[24,25] The band at 1672 cm^{-1} is due to the random structure. It is evident that an increase in concentration brings about an increase in the intensities of both the 1624 and 1692 cm^{-1} bands, indicating an increased population of the β-sheet structure. Thus, it has been concluded for the AN_pZ– and ON_pZ–dioxane (or benzene) solutions that aggregation induces the conformational change from a random structure to an antiparallel-type β-sheet structure which occurs above the c.a.c. and, as a consequence, aggregates are formed through intermolecular hydrogen bonding between the peptide C=O and NH groups. The results obtained from the IR spectra show that preferential stabilization of the antiparallel β-sheet structure occurs upon aggregation.

Furthermore, in this present study, SANS and SAXS measurements for the deuteriated dioxane and benzene solutions

Table 1 Molecular parameters for AN_pZ used for SANS and SAXS spectra

Material	A4Z	A5Z	A6Z	A8Z	A10Z	A12Z	A14Z
Residue number	4	5	6	8	10	12	14
Formula	$C_{57}H_{62}N_4O_{14}$	$C_{69}H_{75}N_5O_{17}$	$C_{81}H_{88}N_6O_{20}$	$C_{105}H_{114}N_8O_{26}$	$C_{129}H_{140}N_{10}O_{32}$	$C_{153}H_{166}N_{12}O_{38}$	$C_{177}H_{192}N_{14}O_{44}$
Molecular weight	1027.1	1246.4	1465.6	1904.1	2342.6	2781.1	3219.5
V/Å^3 [a]	1363.8	1650.1	1928.3	2494.2	3058.7	3623.2	4187.7
H/Å [b]	4.74	4.73	4.71	4.71	4.71	4.71	4.71
ξ [c]	1.00[e]	1.00[e]	1.00[e]	1.00[e]	2.09	2.41	2.74
μ/Å [d]	9.5	10.5	11.5	13.0	10.0	10.0	10.0

[a] Molecular volume calculated from partial molar volume data.[25] [b] Height of a disk (from X-ray diffraction pattern of the solid). [c] Axial ratio of elliptical cylinder (from molecular model). [d] Minor axis or radius of a disk. [e] Calculated from cylindrical model.

Table 2 Molecular parameters for ON_pZ used for SANS and SAXS spectra

Material	O6Z	O8Z	O12Z
Residue number	6	8	12
Formula	$C_{88}H_{102}N_6O_{20}$	$C_{112}H_{128}N_8O_{26}$	$C_{160}H_{180}N_{12}O_{38}$
Molecular weight	1563.7	2002.1	2879.0
V/Å^3 [a]	2125.4	2691.3	3820.3
H/Å [b]	4.68	4.68	4.73
ξ [c]	1.00[e]	1.00[e]	2.41
μ/Å [d]	11.4	13.0	10.0

[a] Molecular volume calculated from partial molar volume data.[25] [b] Height of a disk (from X-ray diffraction pattern of the solid). [c] Axial ratio of elliptical cylinder (from molecular model). [d] Minor axis or radius of a disk. [e] Calculated from cylindrical model.

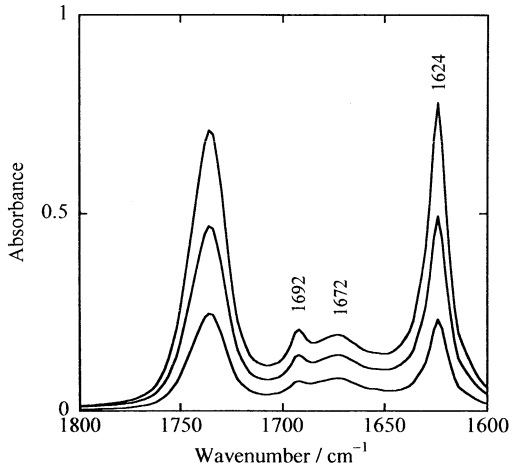

Fig. 1 The FTIR spectra of the A10Z–dioxane solutions (0.013, 0.009 and 0.004 mol l^{-1} from top to bottom) in the 1600–1800 cm^{-1} region.

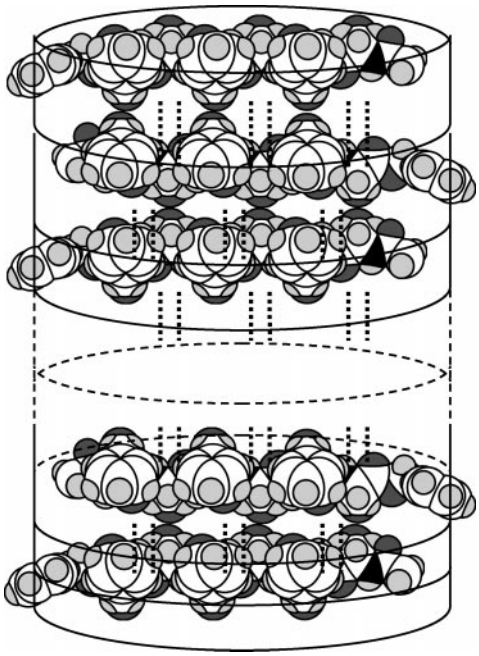

Fig. 2 Schematic model of the A6Z aggregate.

of these oligomers and their spectral analyses have been carried out, in order to obtain detailed information of the shape and size of the aggregates and their growth process.

Structural model of the AN_pZ and ON_pZ aggregates

The following assumptions have been made for analysis of the SANS and SAXS data.

(1) The oligomeric molecules forming the aggregate take up an antiparallel β-sheet structure in solution. The β-sheet oligomers can be regarded as a flat disk.

(2) Formation of intermolecular hydrogen bonding occurs between different disk-like molecules above the c.a.c., leading to a one-dimensional linear model of a rod-like aggregate in which the disk-like oligomers are stacked antiparallel to each other through intermolecular hydrogen bonding (Fig. 2).

(3) The aggregates, in which the monomers are one-dimensionally stacked, are in the polydispersed state.

SANS and SAXS analysis and the extracted results

The SANS spectra of the AN_pZ–dioxane(d8) (N_p = 5, 6, 10, 12 and 14) systems, and the SAXS spectra of the AN_pZ–benzene (N_p = 4, 5, 6 and 8) systems and of the A8Z–dioxane systems were analyzed with the aggregation number (N_n) as a fitting parameter, thus assuming polydispersity and constancy for the remaining molecular parameters. The observed and best fit scattering intensity profiles for the series of AN_pZ are shown in Fig. 3 and 4. The closeness of fit between the observed and calculated results is excellent, indicating that the observed SANS spectra can be explained by a one-dimensional stacked linear model. The fitting parameter [number-average aggregation number (N_n)], extracted number-average molecular weight (M_n), extracted monomer–monomer bond energy ($\alpha\kappa T$), and scaling factor (A) are listed in Tables 3 and 4.

As is shown in Fig. 5[A], for the AN_pZ–benzene systems, as the concentration increases above the c.a.c., the number-average aggregation number (N_n) tends to increase until it finally comes close to a constant value, which depends upon the N_p value (17 for A4Z, 23 for A5Z, 30 for A6Z and 50 for A8Z). For the AN_pZ–dioxane(d8) systems (Fig. 5[B]), the N_n values for A10Z, A12Z and A14Z are almost constant, in the concentration range measured in the present study, although those of A5Z, A6Z and A8Z tend to increase and converge.

For the AN_pZ–dioxane(d8) systems, the $\alpha\kappa T$ value increases with an increase in the residue number for shorter oligomers ($N_p < 8$) and becomes constant for longer oligomers ($N_p \geqslant 8$), although its concentration dependence is very small in the range measured. For the AN_pZ–benzene systems, the residue number and concentration dependence of this energy value are very small.

Effect of water molecules on the aggregational behavior

In order to investigate the effect of water molecules on the aggregational behavior of AN_pZ oligomers, SAXS measurements of the A6Z–(dioxane + water) system with different

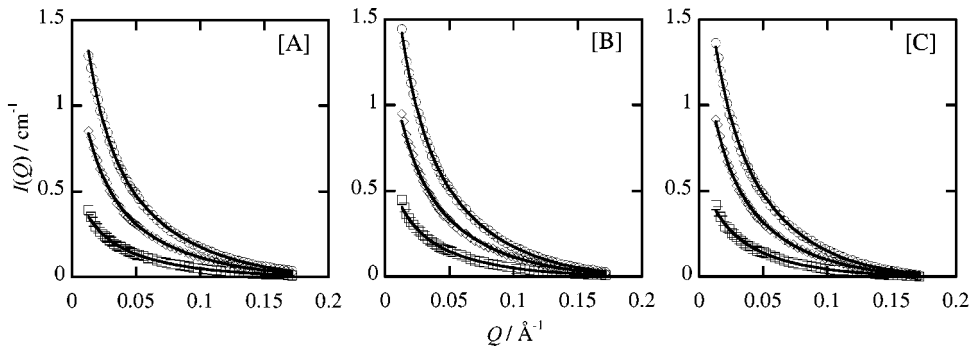

Fig. 3 The observed SANS spectra of the AN_pZ–dioxane(d8) solutions at various concentrations: [A] A10Z (○: 0.015 mol l^{-1}, ◇: 0.010 mol l^{-1} and □: 0.005 mol l^{-1}), [B] A12Z (○: 0.012 mol l^{-1}, ◇: 0.008 mol l^{-1} and □: 0.004 mol l^{-1}) and [C]: A14Z (○: 0.011 mol l^{-1}, ◇: 0.007 mol l^{-1} and □: 0.004 mol l^{-1}); and least squares best fit profiles (solid lines).

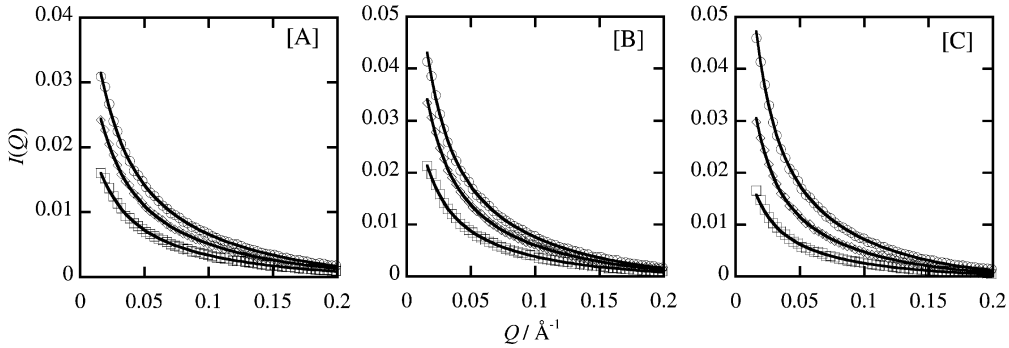

Fig. 4 The observed SAXS spectra of the AN_pZ–benzene solutions at various concentrations: [A] A4Z (○: 0.017 mol l^{-1}, ◇: 0.013 mol l^{-1} and □: 0.009 mol l^{-1}), [B] A5Z (○: 0.014 mol l^{-1}, ◇: 0.011 mol l^{-1} and □: 0.007 mol l^{-1}) and [C] A6Z (○: 0.009 mol l^{-1}, ◇: 0.006 mol l^{-1} and □: 0.003 mol l^{-1}); and least squares best fit profiles (solid lines).

Table 3 Fitted aggregation number (N_n), extracted bond energy (αkT), extracted molecular weight (M_n), and calculated scaling factor (A) for the AN_pZ– and ON_pZ–1,4-dioxane systems

Sample	C/mol l^{-1}	N_n	αkT/kJ mol^{-1}	M_n	A
A5Z	3.6×10^{-2}	2	18	2.5×10^{3}	1.7×10^{-1}
	4.6×10^{-2}	3	19	3.7×10^{3}	2.6×10^{-1}
	5.5×10^{-2}	4	20	5.0×10^{3}	4.4×10^{-1}
A6Z	0.8×10^{-2}	10	30	1.5×10^{4}	3.4×10^{-1}
	1.5×10^{-2}	16	30	2.3×10^{4}	1.3
	2.3×10^{-2}	18	30	2.6×10^{4}	2.3
A8Z	0.5×10^{-2}	23	35	4.4×10^{4}	1.4×10^{-3}
	1.1×10^{-2}	25	33	4.8×10^{4}	3.2×10^{-3}
	1.6×10^{-2}	27	33	5.1×10^{4}	4.9×10^{-3}
A10Z	0.5×10^{-2}	18	34	4.2×10^{4}	4.6×10^{-1}
	1.0×10^{-2}	19	32	4.5×10^{4}	1.1
	1.5×10^{-2}	20	32	4.7×10^{4}	1.8
A12Z	0.4×10^{-2}	19	35	5.3×10^{4}	5.4×10^{-1}
	0.8×10^{-2}	18	33	5.0×10^{4}	1.2
	1.2×10^{-2}	19	32	5.3×10^{4}	1.9
A14Z	0.4×10^{-2}	18	35	5.8×10^{4}	5.1×10^{-1}
	0.7×10^{-2}	19	33	6.1×10^{4}	1.2
	1.1×10^{-2}	18	32	5.8×10^{4}	1.8
O6Z	2.2×10^{-2}	14	29	2.2×10^{4}	1.7
O8Z	1.7×10^{-2}	15	30	3.0×10^{4}	2.1
O12Z	1.2×10^{-2}	16	31	4.6×10^{4}	2.6

Table 4 Fitted aggregation number (N_n), extracted bond (αkT), extracted molecular weight (M_n), and calculated scaling factor (A) for the AN_pZ–benzene systems

Sample	C/mol l^{-1}	N_n	αkT/kJ mol^{-1}	M_n	A
A4Z	0.9×10^{-2}	17	32	1.7×10^{4}	2.3×10^{-2}
	1.3×10^{-2}	17	31	1.7×10^{4}	3.4×10^{-2}
	1.7×10^{-2}	17	30	1.7×10^{4}	4.4×10^{-2}
A5Z	0.7×10^{-2}	22	34	2.7×10^{4}	3.4×10^{-2}
	1.1×10^{-2}	23	33	2.9×10^{4}	5.6×10^{-2}
	1.4×10^{-2}	23	32	2.9×10^{4}	7.1×10^{-2}
A6Z	0.4×10^{-3} [a]	7	35	1.0×10^{4}	7.6×10^{-6}
	1.2×10^{-3} [a]	17	37	2.5×10^{4}	3.0×10^{-5}
	2.8×10^{-3} [a]	24	36	3.5×10^{4}	8.2×10^{-5}
	2.8×10^{-3}	24	37	3.5×10^{4}	2.7×10^{-2}
	6.0×10^{-3}	28	36	4.1×10^{4}	5.7×10^{-2}
	9.0×10^{-3}	30	37	4.4×10^{4}	9.2×10^{-2}
A8Z	0.9×10^{-3} [a]	5	31	9.5×10^{3}	6.2×10^{-6}
	1.4×10^{-3} [a]	18	37	3.4×10^{4}	3.7×10^{-5}
	1.8×10^{-3} [a]	21	37	4.0×10^{4}	5.9×10^{-5}
	2.3×10^{-3} [a]	36	38	6.9×10^{4}	1.3×10^{-4}
	2.3×10^{-3}	44	40	7.6×10^{4}	9.2×10^{-3}
	4.6×10^{-3}	46	37	8.8×10^{4}	1.9×10^{-2}
	7.0×10^{-3}	50	38	9.5×10^{4}	2.9×10^{-2}

[a] SAXS spectra of these solutions were measured by use of the BL-15A line.

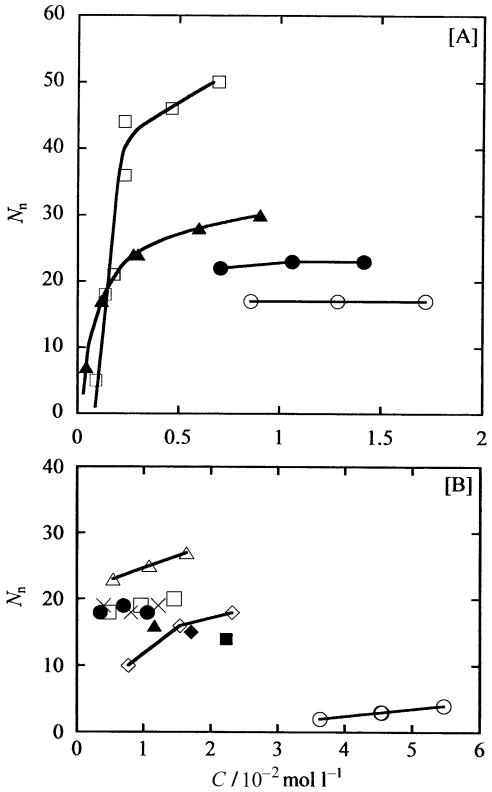

Fig. 5 Concentration dependence of the N_n value [A] for the AN_pZ–benzene systems (□: A8Z, ◆: A6Z, ●: A5Z and ○: A4Z,) and [B] for the AN_pZ–dioxane(d8) systems (◇: A8Z, □ A10Z, ●: A12Z, ●: A14Z, ◇: A6Z, ○: A5Z, ▲: O12Z, ◆: O8Z and ■: O6Z).

H_2O volume fractions ($V_{H_2O}/(V_{dioxane} + V_{H_2O})X = 0.02$, 0.04 and 0.06) and SAXS analyses were carried out (observed and calculated intensity profiles not shown). The number-average aggregation number (N_n), number-average molecular weight (M_n) of an A6Z aggregate and bond energy ($\alpha\kappa T$) were extracted: $N_n = 8$, $M_n = 1.2 \times 10^4$ and $\alpha\kappa T = 26$ kJ mol^{-1} for the A6Z–(dioxane + water) system with $X = 0.02$. As a consequence, it has been found that addition of water induces decreases in the N_n, M_n and $\alpha\kappa T$ values, indicating that water molecules inhibit the formation of hydrogen bonding between the A6Z monomers in dioxane.

Discussion

From the IR, SANS and SAXS spectral results, which have been described for the AN_pZ– and ON_pZ–dioxane or benzene systems in this present paper, it can be concluded that the AN_pZ and ON_pZ oligopeptides in dioxane and benzene form rod-like aggregates, in which the disk-like β-sheet oligomers are one-dimensionally stacked onto each other in an antiparallel manner through intermolecular hydrogen bonding, as shown schematically in Fig. 2.

The origin of this association in an antiparallel manner between neighboring AN_pZ or ON_pZ monomers seemingly comes from the interactions between the electric dipole moments as a result of small peptide dipole moments, which are aligned approximately perpendicular to the molecular axis of a β-sheet molecule. (Thus, the dipole moment of a β-sheet oligopeptide may be considerably smaller than the large one of α-helical PBLG,[26] although the magnitude has not yet been determined.) However, the resultant dipole–dipole interaction does not play a significant role in orienting the β-sheet oligopeptides in an antiparallel manner in the aggregates, since the dipole–dipole interaction acts over a long range. The present solute–solute interaction, that is, the β-sheet–β-sheet interaction, should be a short-range interaction. Indeed, since an increase in the concentration of a solute results in an increased population of the β-sheet stacked aggregates, in dilute solution, the solvent–solute interaction may be dominant, but the solute–solute interaction becomes important when the solution is concentrated.

The driving force for starting such an aggregation pattern may originate from the interaction between the side chains (–$COOCH_2C_6H_5$), which belong to the neighboring β-sheet oligopeptides. For the mechanism of molecular association of the α-helical PBLG in solution, Wada[13] concluded from dielectric data that the binding force may originate from the interaction between the side chains, which belong to the neighboring helices. The existence of the side chain–side chain interaction between the α-helices of L- and D-PBLG chains has been confirmed by Tsuboi *et al.*[27] using the X-ray diffraction patterns of oriented fibers of a 50 : 50 mixture of the D- and L-polypeptides. They suggested that such a side chain–side chain interaction may take place once every two pitches of the α-helix.

The reason why the antiparallel β-sheet oligomers for the AN_pZ or ON_pZ series are stabilized in dioxane solution may be related to the enthalpic difference between the parallel and the antiparallel molecular arrangements. We have no data on such an energy difference for the two conformations. However, judging from the experimental data on other peptides,[27] it may be expected that the enthalpic difference must be very small. The NMR data[28] suggest that partially *N*-methylated derivatives of *cyclo*-D,L-$(Ala)_4(Phe)_4$ peptide in chloroform solution favor the antiparallel structure by 3.36 kJ mol^{-1}. Force field energy minimization studies[29] suggested that the antiparallel β-sheets are slightly more stable than their parallel counterparts. The results,[30] which were calculated for cyclooctapeptides of two peptide chains consisting of 11 amino acid residues (Ala and Gly) using quantum mechanical programs (AMI), showed that the enthalpic difference between the parallel and antiparallel β-sheet arrangements is very small.

For *N*-urethanyl amino acids like *N*-*tert*-Boc-glycine, *N*-*tert*-Boc-L-alanine, *N*-*tert*-Boc-L-methionine, *N*-*tert*-Boc-*O*-Bz-L-tyrosine in chloroform, NMR studies have shown that the *cis* form about the peptide C⁓N bond is favored at room temperature.[31] For the present AN_pZ or ON_pZ oligomers with peptide groups equal to the residue number, there are two possible conformations about each peptide C⁓N bond. When the β-sheet structure of the AN_pZ or ON_pZ molecules is stabilized, all peptide groups should take up the *trans* form about the C⁓N bond.

As described in the Introduction, the hydrophobic interaction of the *N*-acyl chains for the *N*-acylsarcosinate ion induces preferential stabilization of the *trans* form about the peptide C⁓N bond upon micellization.[6] Indeed, below the critical micelle concentration (c.m.c.) the percentage of the *trans* configuration (46%) is less than that of the *cis* isomer (54%). However, it increases asymptotically with further increasing concentration above the c.m.c., and finally approaches the constant value (76%) in the micellar state. Furthermore, the effect of temperature on the population of isomers was also investigated,[7] and the energy barrier to rotation about the C⁓N bond in the monomeric and micellar states was estimated from the results of line shape analysis of the ^{1}H NMR spectra, revealing that the energy difference between the two isomers is extremely small. For the sarcosinate anion with an *N*-octanoyl chain, the apparent activation energies about the C⁓N bond in the monomeric and micellar states were 55.6 and 83.7 kJ mol^{-1}, respectively.

Thus, this concept of stabilization of a specific isomer upon aggregation may apply to the AN_pZ or ON_pZ oligomers. Judging from the amide I mode features of the IR spectra, random forms of these oligopeptides may be predominant in

the diluted solutions below the c.a.c., implying that no preferential stabilization of the *trans* form, for each peptide group, occurs in the monomeric state. However, when the concentration increases above the c.a.c., as soon as the *trans* form, for one of the peptide groups, is stabilized because of the side chain–side chain interaction, stabilization of the *trans* forms for other peptide groups may occur cooperatively, leading to preferential stabilization of the β-sheet.

We may discuss the stacking manner of side chains in the AN_pZ aggregate. Fig. 6 shows the schematic models of the two possible stacking manners between the monomers constituting an aggregate. In the parallel type [A], the interactions between the counterparts may be possible for all phenyl groups containing the C-terminal benzyl groups, while in the antiparallel type [B] all the phenyl groups except the C-terminal group interact with the counterparts. When the antiparallel β-sheet is predominantly stabilized in the aggregates, it may be assumed that a B-type stacking manner is possible in the AN_pZ aggregates. In this stacking manner, although π–π interactions may be possible between the side-chain phenyl groups, the C-terminal phenyl group may interact with the N-terminal acetyl CH_3 group of a counterpart by CH···π interaction. In fact, the existence of the intraligand or intramolecular CH···π interaction was confirmed by Jitsukawa *et al.*[32,33] for binary cobalt(III) complexes of *N*-pyridoxyl-2-amino acid or for ternary metal [Cu(II), Pd(II)] complexes involving *o*-, *m*- or *p*-methyl-substituted phenylalanine and 1,10-phenanthroline using a single crystal X-ray diffraction study.

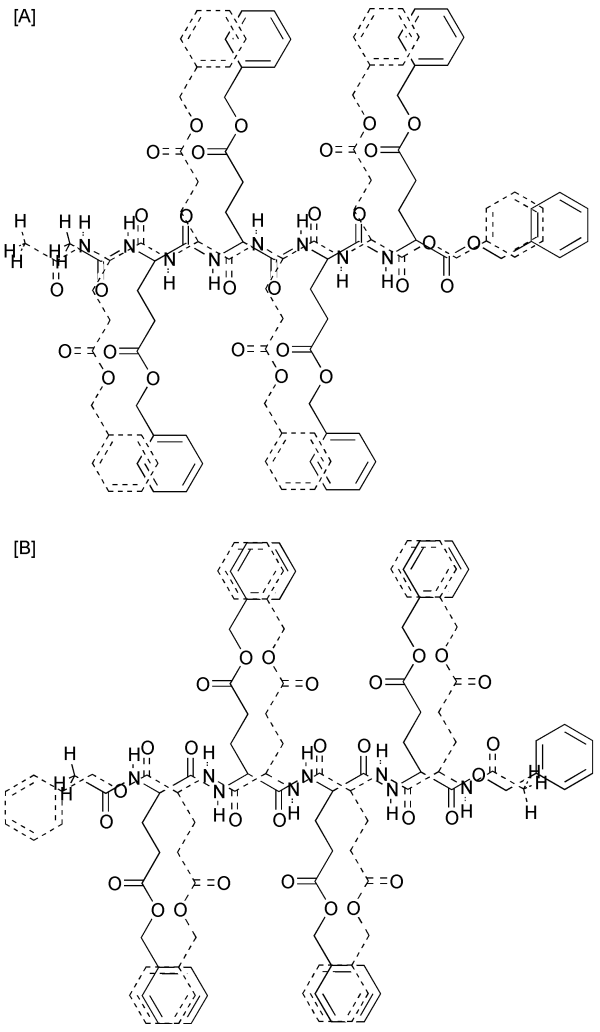

Fig. 6 Schematic models ([A] parallel type and [B] antiparallel type) of the stacking pattern in the A4Z aggregate.

Amino or amide N–H···π(aromatic) interactions have been theoretically postulated in a model system and experimentally described in globular proteins.[34,35] Furthermore, experimental evidence has been presented[36–38] at the level of atomic resolution for intramolecular N–H···π(phenyl) interactions in a family of amino acid derivatives. However, based on the molecular model, the CH···π interactions may favor a one-dimensionally β-sheet stacked aggregate.

In order to obtain evidence of the CH···π interaction, we have measured the concentration dependence of the ^{1}H NMR spectral feature for the A4Z–benzene(d6) system, focusing on the signals of the acetyl CH_3 protons (spectra not shown). The result showed that the CH_3 signal rapidly shifts low-field above the c.a.c. (0.0036 mol l^{-1}), which corresponds to the c.a.c. determined by the ^{1}H NMR method (to be reported separately), and the increase of the half-height width ($\Delta\nu_{1/2}$) occurs above this concentration, showing the appearance of the CH_3···π interaction upon aggregation.

Judged from the dielectric data for the α-helical PBLG–dioxane system,[13,26] which provided results that the side chain should be arranged so that its dipole moment cancels out a part of the moment of the peptide group in the main chain, such an aggregation for AN_pZ or ON_pZ oligomers probably also induces an increase in the extent of ordering of the side chain containing the ester group. For the aggregates in the present oligomeric solutions, the β-sheet structures of the main chain induced by aggregation are further one-dimensionally stacked through relatively strong hydrogen bonding. This may induce increased side chain–side chain interaction, bringing about an increased extent of orientational ordering of the side chain.

As seen in Tables 3 and 4, it is evident that the number-averaged aggregation number (N_n) and the monomer–monomer bond energy ($\alpha\kappa T$) for the AN_pZ aggregates in dioxane are smaller than those in benzene. This fact may be due to the difference in the extent of solvation for AN_pZ molecules between dioxane and benzene. That is, in the AN_pZ–dioxane systems, it may be assumed that formation of weak hydrogen bonding between the peptide NH of the solute and the ether-linkage oxygen (–CH_2–O–CH_2–) of dioxane bring about an increased extent of solvation for an AN_pZ molecule compared with the case in benzene, although the hydrogen bonding potential is very low for dioxane and is almost zero for benzene. This trend may disturb the formation of intermolecular hydrogen bonding between the monomers of AN_pZ (or ON_pZ), leading to a decrease in the aggregation number and the $\alpha\kappa T$ values in dioxane.

It may be accepted that the hydrogen bond is predominantly an electrostatic interaction and that the H atom is not shared but remains closer to and covalently bound to its parent atom (X),[39] as usually denoted by X–H···Y. The strength of most hydrogen bonds[21] is in the energy range of 10–40 kJ mol^{-1}, which makes them stronger than a typical van der Waals force (~1 kJ mol^{-1}). All the $\alpha\kappa T$ values obtained for the AN_pZ or ON_pZ systems are approximately in this energy range and are exactly equal to the hydrogen bond energies. Therefore, we can regard the $\alpha\kappa T$ value as an indicator of the strength of hydrogen bonds between the AN_pZ (or ON_pZ) monomers.

Moreover, we should note for the AN_pZ–dioxane systems that the aggregation number rapidly increases with an increase in residue number (N_p) below $N_p = 8$ and that it comes close to the constant aggregation number above this residue number. This fact indicates that the molecular size (length) of the AN_pZ oligomer limits the size (aggregation number) of the aggregate. We may now discuss the reason why the chain length of the oligomer limits the aggregation number.

Fig. 7 shows the plot of the $\alpha\kappa T$ value per peptide residue ($\alpha\kappa T/N_p$) against the residue number (N_p) for the

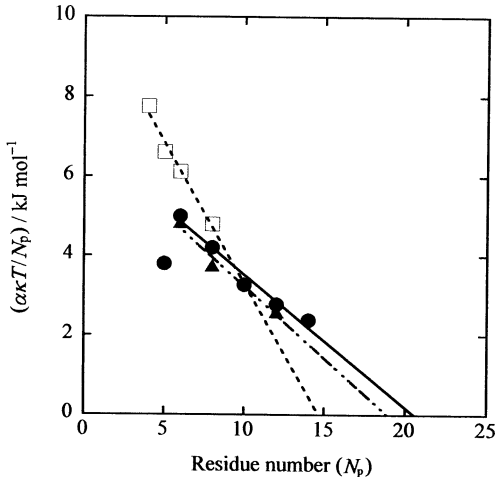

Fig. 7 Plots of the monomer–monomer bond energies per peptide residue ($\alpha\kappa T/N_p$) against the residue number (N_p) for the AN_pZ–dioxane(d8) (●), ON_pZ–dioxane(d8) (◆) and AN_pZ–benzene(d6) (□) systems.

AN_pZ–benzene and AN_pZ–dioxane systems. The $\alpha\kappa T$ values, which were calculated from the small angle scattering intensity data of the most concentrated sample solution for each oligomer, were used for this plotting. It should be noted that there is a linear relationship between $\alpha\kappa T/N_p$ and N_p, implying that the energy of hydrogen bonds per residue between the monomer and the monomer in the aggregate decreases linearly with an increase in residue number. From this linear relationship, we can estimate the number of peptide residues at $\alpha\kappa T/N_p = 0$, by extrapolating the $\alpha\kappa T/N_p$ value to zero. For the AN_pZ–dioxane and ON_pZ–dioxane systems, the $\alpha\kappa T/N_p$ value becomes zero at $N_p \approx 21$ and 19, respectively, while for the AN_pZ–benzene system it becomes zero at $N_p \approx 15$. Therefore, we may estimate from these results that the energy of intermolecular hydrogen bonds in the AN_pZ and ON_pZ aggregates becomes zero at a residue number of *ca.* 20 in dioxane, while that of the aggregate in benzene becomes zero at $N_p \approx 15$, implying that the contribution of intermolecular hydrogen bonding to the formation of the rod-like aggregate, in which the flat β-sheet oligomers are one-dimensionally stacked in an antiparallel manner, becomes very low or zero at these residue numbers. That is, for the AN_pZ and ON_pZ oligomers with these high residue numbers ($N_p > 14$), the aggregation number most probably becomes very small.

The residue numbers, 15–20, in the AN_pZ or ON_pZ systems may be very close to the critical residue number for taking up an α-helical conformation. Therefore, we may assume that, as the residue number of these oligopeptides further increases, the β-sheet structure becomes unstable, resulting in a decrease in the $\alpha\kappa T/N_p$ value. Moreover, the increase in the chain length probably makes possible the twist type of β-sheet structure, and finally the conformation of each monomer changes from a β-sheet to an α-helix, leading to the association of the α-helices.

It is well known that identical tandem repeats of oligopeptides[40] or non-tandem identical repeats[41] exist in proteins, although very little is known about the biological role of the repeating oligomers. In particular, the so-called super-secondary structures, formed by repeating units of the oligopeptides, may have a significant, presently undefined, biological function. Studies on the super-secondary structure (that is, supramolecular structure) of the AN_pZ or ON_pZ series, which can also be regarded as a model system of such repeating oligopeptides, will provide basic and important contributions to the understanding of the super-secondary structure of proteins, which at present remains largely unresolved.

Conclusion

For the series of AN_pZ ($N_p = 4$, 5, 6, 8, 10, 12 and 14) and ON_pZ ($N_p = 6$, 8 and 10) in dioxane or benzene, predominant stabilization of the antiparallel β-sheet conformation occurs upon aggregation.

The IR, SANS and SAXS spectral analyses provide a linear model of the rod-like aggregate, in which the disk-like β-sheet oligopeptides are one-dimensionally stacked antiparallel to each other through intermolecular hydrogen bonding. We may regard these rod-like aggregates as supramolecular aggregates.

As a consequence of the SANS and SAXS analyses, the number-average aggregation number (N_n), number-average molecular weights (M_n) of an aggregate and the monomer–monomer bond energy ($\alpha\kappa T$), which corresponds to the hydrogen bonding energy between the monomers, were obtained.

It has been found that there exists a linear relationship between the bond energy per peptide residue ($\alpha\kappa T/N_p$) and the residue number (N_p). From this linear relationship, we were able to estimate that the contribution of intermolecular hydrogen bonding to the formation of the one-dimensionally stacked rod-like aggregate becomes very low or zero with a further increase in residue number and that such an aggregate structure, consisting of β-sheet monomers, may be broken at $N_p > 14$.

References

1 H. Okabayashi, M. Okuyama and T. Kitagawa, *Bull. Chem. Soc. Jpn.*, 1975, **48**, 2264.
2 H. Okabayashi and M. Abe, *J. Phys. Chem.*, 1980, **84**, 999.
3 H. Okabayashi, T. Yoshida, T. Ikeda, H. Matsuura and T. Kitagawa, *J. Am. Chem. Soc.*, 1982, **104**, 5399.
4 K. Tsukamoto, K. Ohshima, T. Taga, H. Okabayashi and H. Matsuura, *J. Chem. Soc., Faraday Trans. 1*, 1987, **83**, 789.
5 H. Okabayashi, K. Tsukamoto, K. Ohshima, T. Taga and E. Nishio, *J. Chem. Soc., Faraday Trans. 1*, 1988, **84**, 1639.
6 H. Takahashi, Y. Nakayama, H. Hori, K. Kihara, H. Okabayashi and M. Okuyama, *J. Colloid Interface Sci.*, 1976, **54**, 102.
7 H. Okabayashi, K. Kihara and M. Okuyama, in *Colloid and Interface Science*, ed. M. Kerker, R. L. Rowell and A. C. Zettlemoyer, Academic Press, New York, 1976, vol. II, p. 357.
8 E. L. Becker, H. E. Bleich, A. R. Day, R. I. Frear, J. A. Ghasel and J. Vinsintainner, *Biochemistry*, 1979, **16**, 4656.
9 M. N. G. James, G. D. Brayer, L. T. T.-J. Delbaire, A. R. Sielecki and A. Gertler, *J. Mol. Biol.*, 1980, **139**, 423.
10 N. V. Beaudette, A. W. Flumer, H. Okabayashi and G. D. Fasman, *Biochemistry*, 1981, **20**, 6526.
11 N. V. Beaudette, H. Okabayashi and G. D. Fasman, *Biochemistry*, 1982, **21**, 1765.
12 (*a*) P. Doty, J. H. Bradbury, A. M. Holtzer and E. R. Blout, *J. Am. Chem. Soc.*, 1954, **76**, 4493; (*b*) P. Doty, J. H. Bradbury and A. M. Holtzer, *J. Am. Chem. Soc.*, 1956, **78**, 947.
13 A. Wada, *J. Polym. Sci.*, 1960, **45**, 145.
14 R. Tadmor, A. Dagan and Y. Cohen, *Macromol. Symp.*, 1997, **114**, 13.
15 M. R. Ghadiri, J. R. Granja, R. A. Milligan, D. E. McRee and N. Khazanovich, *Nature*, 1993, **366**, 324.
16 G. P. Lorenzi, H. Jäckle, L. Tomasic, V. Rizzo and C. Pedone, *J. Am. Chem. Soc.*, 1982, **104**, 1728.
17 M. R. Ghadiri, J. R. Granja and L. K. Buehler, *Nature*, 1994, **369**, 301.
18 T. Uehara, H. Okabayashi, T. Taga, T. Yoshida and H. Kojima, *J. Chem. Soc., Faraday Trans.*, 1991, **88**, 3451.
19 S. Vass, T. Torok, G. Jakli and E. Berecz, *J. Phys. Chem.*, 1989, **93**, 6553.
20 V. F. Sears, in *Methods of Experimental Physics*, ed. K. Sköld and D. L. Price, Academic Press, Orlando, FL, 1989, vol. 93, p. 521.
21 *Intermolecular and Surface Forces*, ed. N. J. Israelachivili, Academic Press, New York, 2nd edn., 1991, ch. 16, p. 341.
22 T. Uehara, H. Hirata, H. Okabayashi, T. Taga, T. Yoshida and H. Kojima, *Colloid Polym. Sci.*, 1994, **272**, 692.
23 T. Imae and S. Ikeda, *Mol. Cryst. Liq. Cryst.*, 1981, **65**, 73.
24 Y. Masuda and T. Miyazawa, *Macromol. Chem.*, 1967, **103**, 261.
25 T. Miyazawa and E. R. Blout, *J. Am. Chem. Soc.*, 1961, **83**, 712.

26 A. Wada, *J. Chem. Phys.*, 1959, **31**, 495.
27 M. Tsuboi, A. N. Wada and N. Nagashima, *J. Mol. Biol.*, 1961, **3**, 705.
28 M. R. Ghadiri, K. Kobayashi, J. R. Granja, R. K. Chandha and D. E. McRee, *Angew. Chem., Int. Ed. Engl.*, 1995, **34**, 93.
29 (*a*) M. Vásquez, G. Némethy and H. A. Sheraga, *Chem. Rev.*, 1994, **94**, 2183; (*b*) K.-C. Chou, G. Némethy and H. A. Sheraga, *J. Mol. Biol.*, 1983, **168**, 389; (*c*) K.-C. Chou, G. Némethy and H. A. Sheraga, *Biochemistry*, 1983, **22**, 6213; (*d*) F. R. Salemme and D. W. Weatherford, *J. Mol. Biol.*, 1981, **146**, 101; (*e*) F. R. Salemme, *J. Mol. Biol.*, 1981, **146**, 143.
30 C. Gailer and M. Feigel, *J. Comput.-Aided Mol. Design*, 1997, **11**, 273.
31 (*a*) M. Branik and H. Kessler, *Chem. Rev.*, 1973, **108**, 2176; (*b*) A. C. Chernovitz, T. B. Friedman and L. A. Nafie, *Biopolymers*, 1987, **26**, 1879.
32 (*a*) K. Jitsukawa, K. Iwai, H. Masuda, H. Ogoshi and H. Einaga, *Chem. Lett.*, 1994, **2**, 303; (*b*) K. Jitsukawa, K. Iwai, H. Masuda, H. Ogoshi and H. Einaga, *J. Chem. Soc., Dalton Trans.*, 1997, 3691.
33 M. Mizutani, S. Tomosue, H. Kinoshita, K. Jitsukawa, H. Masuda and H. Einaga, *Bull. Chem. Soc. Jpn.*, 1999, **72**, 981.
34 M. Levitt and M. F. Perutz, *J. Mol. Biol.*, 1988, **201**, 751.
35 J. B. O. Mitchell, C. L. Nandi, I. K. McDonald, J. M. Thornton and S. L. Price, *J. Mol. Biol.*, 1994, **239**, 315.
36 G. Valle, M. Crisma, C. Toniolo, N. Sen, M. Sukumar and P. Balaram, *J. Chem. Soc., Faraday Trans.*, 1988, **2**, 373.
37 H. Kumita, K. Jitsukawa, H. Masuda and H. Einaga, *J. Inorg. Biochem.*, 1997, **67**, 295.
38 M. Crisma, F. Formaggio, G. Valle, C. Toniolo, M. Saviano, R. Iacovino, L. Zaccaro and E. Benedetti, *Biopolymers*, 1997, **42**, 1.
39 H. Umeyama and K. Morokuma, *J. Am. Chem. Soc.*, 1977, **99**, 1316.
40 A. Esen, J. Bietz, A, J. W. Paulis and J. S. Wall, *Nature*, 1982, **296**, 678.
41 S. Isemura, E. Saito and K. Sanada, *J. Biochem.*, 1980, **87**, 1071.